

Provably Uncertainty-Guided Universal Domain Adaptation

Yifan Wang, Lin Zhang, Ran Song, and Wei Zhang

Abstract—Universal domain adaptation (UniDA) aims to transfer the knowledge of common classes from source domain to target domain without any prior knowledge on the label set, which requires to distinguish the unknown samples from the known ones in the target domain. A main challenge of UniDA is that the unequal label spaces of both domains causes the misalignment between two domains. Moreover, the domain discrepancy and supervised objectives in source domain lead the whole model to be biased towards the common classes and produce the overconfident predictions for unknown samples. To address the above challenging problems, we propose a new uncertainty-guided UniDA framework. Firstly, we introduce an empirical estimation of the probability of a target sample belonging to the unknown class with exploiting the distribution of target samples. Then, based on the estimation, we propose a novel neighbors searching method in the linear subspace with a δ -filter to estimate the uncertainty score of a target sample and discover unknown samples. It fully utilizes the relationship between a target sample and its neighbors in source domain to avoid the influence of domain misalignment. Secondly, this paper well balances the confidence of predictions for both known and unknown samples through an uncertainty-guided margin loss based on the predictions of discovered unknown samples, which can reduce the gap between intra-class variance of known classes with respect to the unknown class. Finally, experiments on three public datasets demonstrate that our method significantly outperforms existing state-of-the-art methods.

Index Terms—Domain Adaptation, Transfer Learning and Representation Learning



1 INTRODUCTION

Unsupervised domain adaptation (UDA) [1], [2], [3], [4], [5] aims to transfer the learned knowledge from the labeled source domain to the unlabeled target domain so that the inter-sample affinities in the latter can be properly measured. The assumption of traditional unsupervised DA, i.e., closed-set DA, is that the source domain shares identical label set with the target domain, which significantly limits its applications in real-world scenarios. Thus, relaxations to this assumption have been investigated. Partial-set DA (PDA) [6], [7], [8], [9] assumes that target domain is not identical to source domain but its subset. On the contrary, Open-set DA (ODA) [10], [11], [12] assumes that target domain contains classes *unknown* to the source domain such that the source domain is a subset of the target domain. Open-partial DA (OPDA) [13], [14], [15] introduces private classes in both domains respectively, where the private classes in the target domain are unknown, and assumes that the common classes shared by the two domains have been identified. As illustrated in Fig. 1(a), Universal DA (UniDA) [13], [14], [16] concerns about unsupervised DA with the most general setting, where no prior knowledge is required on the label set relationship between domains.

A main challenging problem of all UDA problems is the domain misalignment caused by the biased and less-discriminative embedding. The misalignment can easily mislead the knowledge transformation and lead to the incorrect classification. In UniDA problem, the label spaces of two domains are not exactly overlapped which magnifies the domain bias. Thus, besides the misalignment between source and target common samples, another main challenge of UniDA is how to distinguish the unknown target samples.

To deal with the above problem, a popular method [14], [17], [18] is to complete the alignment between samples in common classes of both source and target domains and push the unknown samples away from common classes. For instance, Saito *et al.* [17] proposed a prototype-based method to move each target sample either to a prototype of a source class or to its neighbors in target domain. Li *et al.* [14] solved this problem by replacing the classifier-based framework with a clustering-based one which exploited the intrinsic structure of samples and thus increased the inter-sample affinity in each cluster. Chen *et al.* [18] proposed a geometric anchor-guided adversarial and contrastive learning framework with uncertainty modeling which achieved the state-of-the-art (SOTA) by making samples from each domain closer to their neighbors in both source and target domains.

However, without any prior knowledge about unknown samples and source private classes, approaches [14], [17], [18] of completing the alignment between two domains are dangerous which can even magnify the misalignment. As illustrated in the left part in Fig. 1(b), compared to the inter-sample affinity in a known object class, that in the unknown class can be semantically much larger as the unknown class can contain samples that semantically belong to different object classes especially when the unknown set is large. This means that the inter-sample affinity between two samples in the unknown class could be even lower than that between a sample in the unknown class and a sample in a known object class. Moreover, due to the less-discriminative embedding, the inter-sample affinity between a known sample and unknown samples can be greater than that between it and samples in the same source class. As a result, some unknown samples could be easily pushed closer to one of the

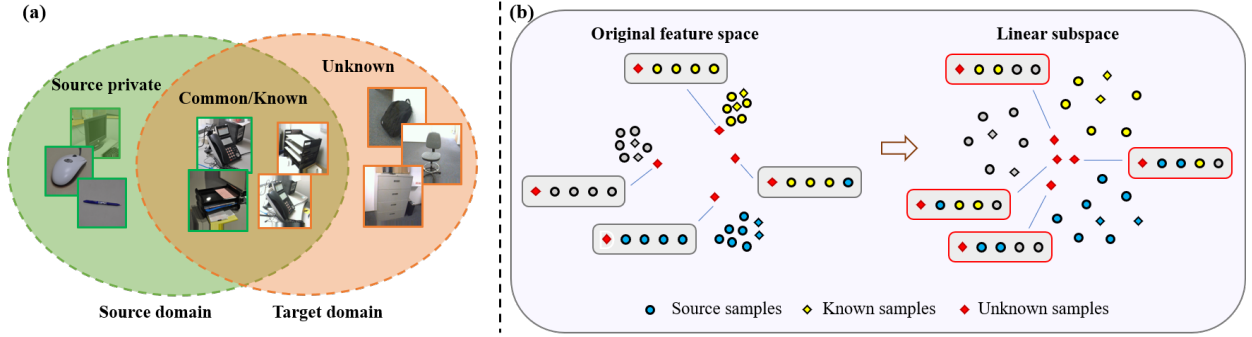


Fig. 1. (a) Illustration of Universal domain adaptation. (b) Given images from two domains, different colors of rims represent different source classes expect the red rim which represents the unknown class.

source classes incorrectly and some known samples can be clustered with the unknown samples which can aggravate the domain misalignment. Thus, it is dangerous to complete the domain alignment without any prior knowledge about the distribution of unknown samples.

Moreover, there is another challenging problem of UniDA. The biased classifier can produce the overconfident predictions for unknown samples which leads to the bad performance. Most of UniDA methods employ one or more classifiers which produce a confidence of each target sample to determine whether it belongs to a particular known class seen in the source domain or the unknown class. Since they usually train their classifiers with the supervised source samples, the less-discriminative embeddings of target samples and labeled objective in source domain can lead the whole model to be biased towards the common classes of target domain, which can make the predictions of many samples belonging to the unknown class overconfident. Moreover, as mentioned by Chen *et al.* [18], the class competition nature may also cause the neural network to generate overconfident predictions for unknown instances. To deal with that, some recent approaches applied extra parameters to help classify the unknown samples, like Fu *et al.* [15] employed multiple classifiers to detect the target “unknown” samples by a mixture of uncertainties, Saito *et al.* [13] proposed to use an One-vs-All classifier to distinguish the unknown samples and Chen *et al.* [18] extended the softmax-based classifier to produce an energy-based uncertainty to determine the unknown samples.

To address the above two issues, we propose a novel uncertainty-guided UniDA framework to reduce the influence of the domain misalignment and balance the confidences of known and unknown samples to deliver a better classification performance. Firstly, without relying on the predictions output by the classifier, we introduce a novel empirical estimation of the posterior probability of a target sample being ‘unknown’ through its the neighborhood information in the source domain. And we prove that the proposed estimation is reliable theoretically. Based on the estimation of the posterior probability, it reveals that the consistency of the labels of neighbors searched from source domain and the distance between the target and its k -nearest neighbor are two keys to distinguish the known and unknown samples. Then, based on these two factors, we propose a novel neighbors searching scheme in the linear subspace with a δ -filter to estimate the uncertainty

of each target sample which is employed to distinguish the the known and unknown samples. Firstly, to better discover unknown samples through the label-consistency of a target sample’s neighbors. We project the features of source and target samples into a linear feature subspace to reduce the influence of the domain misalignment and improve the reliability of neighbors. As illustrated in right part in Fig. 1(b), projecting features in the original representational space into the linear subspace can reduce the correlation of every two samples, which can make the unknown samples away from the edge of source clusters and improve the consistency of the labels of neighbors for an unknown sample decreases. Moreover, since the distance between a known sample and the centroid of a source class would not be significantly different from that between an unknown sample with the centroid, it is hard to find an optimal threshold to filter the discovered known samples through the k -nearest neighbor distance. Therefore, we propose to estimate the difference of the dispersion of two vector set respectively. One set contains the one target sample and its most neighbors belonging to the same class and another set consists of there neighbors and a randomly selected sample from the same source class. The δ -filter can well estimate that if a target sample is compact enough with its most neighbors with the same label.

For the second challenging problem, the classifier training on supervised source samples can be biased to the source classes which can lead to the inconsistency between intra-class variances of source domain and known/unknown target samples. Then it produces overconfident predictions for unknown samples. To deal with that issue, we propose a novel uncertainty-guided margin loss (UGM) to encourage a similar intra-class variances of source domain to that of target domain and discovered unknown samples by enforcing an uncertainty-guided margin to source samples in the current batch. The margin is defined based on the confidence level of unknown samples. A uniform loss is employed to generate a uniform class posterior distribution for discovered unknown samples to increase the entropy of the prediction.

- We introduce an empirical estimation for the posterior probability of a target sample belonging to the unknown class which exploits the distribution of target samples in the latent representational space and theoretically prove the reliability of the proposed empirical estimation.

- Based on the estimation of the posterior probability, we propose a novel neighbors searching method in the linear subspace with a δ -filter where features in the linear subspace can reduce the misalignment between source samples and unknown samples and the δ -filter can determine if a target samples is compact enough with its neighbors.
- We present a novel uncertainty-guided margin loss to balance the intra-class variances between source and target domains which can balance problem between the prediction of known samples and that of unknown samples.
- We perform experiments under various benchmarks. The results demonstrate that our method can significantly outperform baseline methods and achieve state-of-the-art performance on multiple public datasets.

2 RELATED WORK

We briefly review recent unsupervised DA methods in this section. According to the assumption made about the relationship between the label sets of different domains, we group these methods into three categories, namely PDA, ODA and UniDA. We also briefly review a related problem named Out-of-Distribution detection to illustrate the relationship with our work.

2.1 Partial-set Domain Adaptation

PDA requires that the source label set is larger than and contains the target label set. Many methods for PDA have been developed [6], [7], [8], [9], [19]. For example, Cao *et al.* [19] presented the selective adversarial network (SAN), which simultaneously circumvented negative transfer and promoted positive transfer to align the distributions of samples in a fine-grained manner. Zhang *et al.* [8] proposed to identify common samples associated with domain similarities from the domain discriminator, and conducted a weighting operation based on such similarities for adversarial training. Cao *et al.* [7] proposed a progressive weighting scheme to estimate the transferability of source samples. Liang *et al.* [9] introduced balanced adversarial alignment and adaptive uncertainty suppression to avoid negative transfer and uncertainty propagation.

2.2 Open-set Domain Adaptation

ODA, first introduced by Busto *et al.* [10], assumes that there are private and common classes in both source and target domains, and common class labels are known as prior knowledge. They introduced the Assign-and-Transform-Iteratively (ATI) algorithm to address this challenging problem. Recently, one of the most popular strategies [12], [20] for ODA is to draw the knowledge from the domain discriminator to identify common samples across domains. Saito *et al.* [11] proposed an adversarial learning framework to obtain a boundary between source and target samples whereas the feature generator was trained to make the target samples far from the boundary. Bucci *et al.* [16] employed self-supervised learning technique to achieve the known/unknown separation and domain alignment.

2.3 Universal Domain Adaptation

UniDA, first introduced by You *et al.* [21] is subject to the most general setting of unsupervised DA, which involves no prior knowledge about the difference on object classes between the two domains. You *et al.* also presented an universal adaptation network (UAN) to evaluate the transferability of samples based on uncertainty and domain similarity for solving the UDA problem. However, the uncertainty and domain similarity measurements are sometimes not robust and sufficiently discriminative. Thus, Fu *et al.* [15] proposed another transferability measure, known as Calibrated Multiple Uncertainties (CMU), estimated by a mixture of uncertainties which accurately quantified the inclination of a target sample to the common classes. Li *et al.* [14] introduced Domain Consensus Clustering (DCC) to exploit the domain consensus knowledge for discovering discriminative clusters on the samples, which differed the unknown classes from the common ones. OVA_{Net} [13], proposed by Saito *et al.*, trained a one-vs-all classifier for each class using labeled source samples and adapted the open-set classifier to the target domain. Recently, Chen *et al.* [18] proposed a geometric anchor-guided adversarial and contrastive learning framework with uncertainty modeling and achieve the state-of-the-art (SOTA) by exploring a new neighbors clustering method to complete the domain alignment and extend the traditional softmax-based classifier to the energy-based classifier. However, all recent method ignore that adapting the domain misalignment between two domains are dangerous since we do not have any knowledge about the source private classes and the unknown target samples. Especially, they could not perform well in the scenario of the unknown set being large.

2.4 Out-of-Distribution Detection

The problem of detecting outliers and anomalies in the data has been extensively studied in machine learning and signal processing communities which is closely related to outlier detection, a topic that has been greatly studied both in the supervised [22] and unsupervised [23] settings. For unsupervised [23] settings, it is close to UniDA which should detect the unknown samples. To get some inspirations, we mainly focus on the recent deep learning based approaches with unsupervised settings. These methods either estimate the distribution of ID samples [24], [25] or use a distance metric between the test samples and ID samples to detect OOD samples [26], [27]. Many of the existing approaches employ the OOD datasets during training [28], [29] or validation steps [24], [25], [26], [30], [31], [32]. For instance, in [28], the network is fine-tuned during the training to decrease the inter-sample affinity between ID and OOD distributions. Other interesting methods, such as [24], [26], [30], apply a perturbation on each sample at test time to exploit the robustness of their network in detecting ID samples. However, they use part of the OOD samples to fine-tune the perturbation parameters. On the other hand, methods that rely on generative models or auto-encoders, such as Pidhorskyi *et al.* [25], also require hyper-parameters tuning for loss terms, regularization terms, and/or latent space size. Authors in [33] propose to use extra supervision, to construct a better latent space and to detect OOD samples

with high accuracy. Having access to extra information certainly helps with the performance. However, it can be argued that OOD detectors should be completely agnostic of unknown distributions, which is a more realistic scenario in the wild. On the other hand, only a few approaches, such as [27], [34], [35], [36], [37], do not require the OOD samples neither during training nor validation. For instance, Hendricks *et al.* and Gimpel *et al.* [27] show how the softmax layer can be used to detect OOD samples, when its prediction score is below a threshold. In [37], the authors rely on reconstructing the samples to produce a discriminative feature space. However, methods that rely on either reconstruction or generation [25], [36], [37] do not perform well in scenarios where sample generation or reconstruction is more difficult, such as large-scale datasets or video classification. While the problem of detecting OOD samples in image classification has been subject of many studies, in the human action classification domain the focus has been on zero-shot and few shot learning [38].

3 METHOD

In this section, we first introduce the preliminaries of UniDA. Then we introduce an empirical estimation of the probability of a target sample belonging to the unknown class and the unknown samples discovering scheme in linear subspace. Finally, we elaborate the major components of our method in the training process which sufficiently avoids the influence of the domain misalignment and balances the confidences of known and unknown samples.

3.1 Preliminaries

We first establish preliminaries related to our method. Assume that we have the labeled set of source samples $Z^s = \{\mathbf{z}_i^s\}_{i=1}^{N_s}$ defined with the known space of the source label set Y^s and the unlabeled set of target samples $Z^t = \{\mathbf{z}_i^t\}_{i=1}^{N_t}$ where N_s and N_t indicate the numbers of the source and the target samples, respectively. Since the label spaces of the two domains are not aligned, we have the space of the source label set Y^s containing C classes and the target label set $Y^t = Y^{com} \cup Y^{unk}$. Y^{com} and Y^{unk} denote the spaces for the common label set and the unknown label set respectively and we denote the unknown class as $C + 1$ class. With the training on both domains and testing on target domain, our goal is to learn an optimal classifier $D : Z^t \rightarrow Y^s$ to categorize a target sample into an source class belonging to Y^s and distinguish the unknown samples with the entropy of the prediction. Thus, it is important to identify the unknown samples in target domain.

3.2 Empirical Estimation of Unknown Samples

In this section, we introduce an empirical estimation of the posterior probabilities of unknown samples by leveraging the neighborhood information of target data which can distinguish most of the unknown samples more reliably. Theoretically we prove that our empirical estimation of the posterior probability $p(y = C + 1 | \mathbf{z})$ is reliable. Unlike most existing methods [13], [15], [17], [21] relying on the posterior probability of a softmax-based classifier, we focus on the

how target samples distribute in the latent representational space which is shared with source samples.

Proposition 1 *With the feature set of samples from two domains Z^s and Z^t and a target features $\mathbf{z} \in Z^t$. If $\hat{p}_{C+1}(\mathbf{z}; k) = c_1 \mathbb{1}\{\max_{i=0, \dots, C} \hat{p}_i(\mathbf{z}; k, k_i | y = i) \leq \beta\}$ where k and k_i are the number of neighbors and the number of neighbors belonging to class i , respectively. We have:*

$$\text{If} \quad c_0 \frac{k_{max}}{k(r_k)^{m-1}} \leq \beta \quad (1)$$

Then,

$$\mathbb{1}\{p(y = C + 1 | \mathbf{z}) < \gamma\} = \mathbb{1}\{(r_k)^{m-1} < \frac{\epsilon c_0 \gamma}{(1 - \gamma)(1 - \epsilon)}\} \quad (2)$$

where $k_{max} = \max_{i=0, \dots, C} (k_i)$, r_k is the k -nearest neighbor distance, $\gamma \in [0, 1]$ and $c_{0,1}, \epsilon$ are non-zero constants. All samples in the feature space are normalized.

Proof We provide the proof sketch to show our key ideas which revolves around performing the empirical estimation of $p(y = C + 1 | \mathbf{z})$.

First, since we have no idea which known class is the source private class, we denote:

$$p(y = C + 1 | \mathbf{z}) = 1 - p(y \in Y^s | \mathbf{z}) \quad (3)$$

we estimate the posterior distribution of \mathbf{z} belonging to one of source classes which is easier.

By the Bayesian rule, the probability of \mathbf{z} belonging to one of the source classes can be found as:

$$\begin{aligned} p(y \in Y^s | \mathbf{z}) &= \frac{p(\mathbf{z} | y \in Y^s) \cdot p(y \in Y^s)}{p(\mathbf{z})} \\ &= \frac{\sum_{i=0}^C p_i(\mathbf{z}) \cdot \sum_{j=0}^C p(y = j)}{\sum_{i=0}^C p_i(\mathbf{z}) \cdot \sum_{j=0}^C p(y = j) + p_{C+1}(\mathbf{z}) \cdot p(y = C + 1)} \end{aligned} \quad (4)$$

Then, the estimation of the $p(y \in Y^s | \mathbf{z})$ can boil down to deriving the estimations of probability density functions $p_0(\mathbf{z}), \dots, p_{C+1}(\mathbf{z})$

Lemma 2 *With k, k_i and r_k defined in Proposition 1, we can estimate the probability density function $p_i(\mathbf{z})$ as:*

$$\hat{p}_i(\mathbf{z}; k, k_i) = c_0 \frac{k_i}{k(r_k)^{m-1}} \quad (5)$$

Proof Then, since $\mathbf{z} \in \mathbb{R}^m$ and all features are normalized where $\|\mathbf{z}\| = 1$, all data points locate on the surface of a m -dimensional unit sphere. We set $U_r(\mathbf{z}) = \{\|\mathbf{z}' - \mathbf{z}\|_2 \leq r\} \cap \{\mathbf{z}' \in Z^s\}$, which is a set of data points from source domain on the unit hypersphere centered in the \mathbf{z} with a radius r . Assuming the density probability functions satisfy Lebesgue's differentiation theorem, the probability density function can be attained by:

$$p_i(\mathbf{z}) = \lim_{r \rightarrow 0} \frac{p(\mathbf{z}' \in U_r(\mathbf{z}, r) | y = j)}{|U_r(\mathbf{z})|} \quad (6)$$

Then, we denote r_k as the k -nearest neighbor distance which means the r_k Euclidean distance away from center \mathbf{z} and its k -th nearest neighbor. Then we get:

$$\hat{p}_i(\mathbf{z}; k) = \frac{p(\mathbf{z}' \in U_{r_k}(\mathbf{z}) | \mathbf{z}' \in Z_i^s)}{|U_{r_k}(\mathbf{z})|} \quad (7)$$

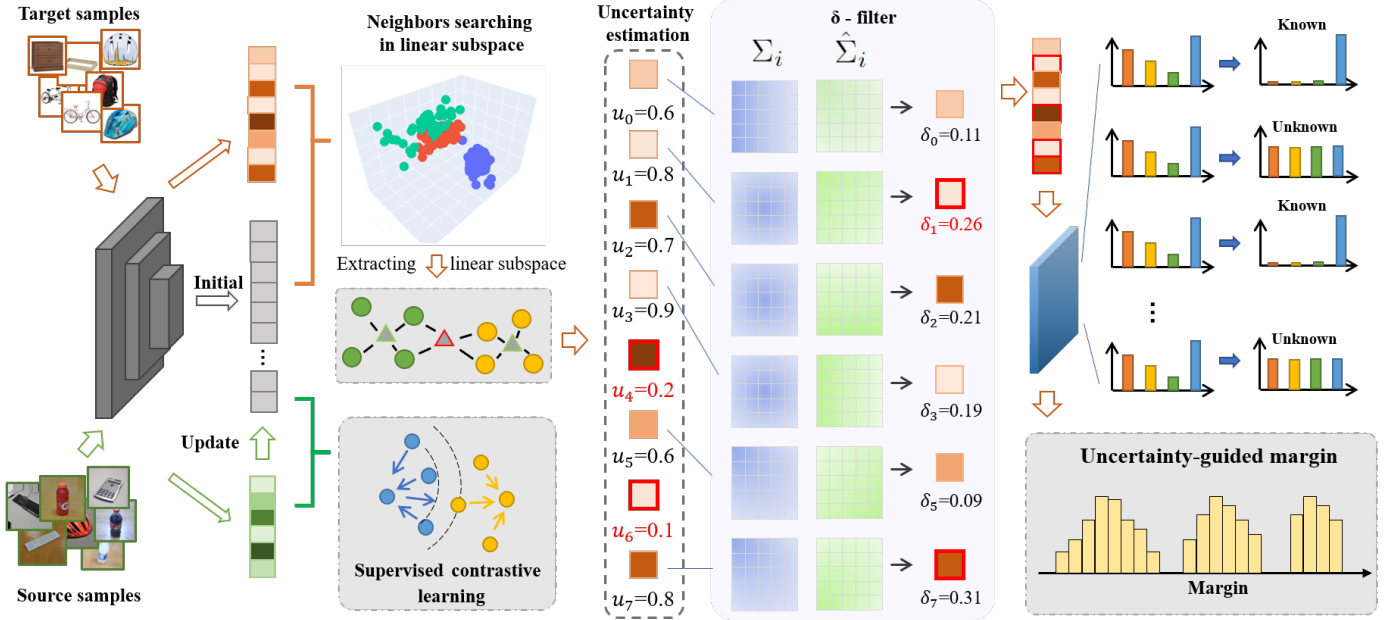


Fig. 2. The overall workflow of the proposed UniDA framework. By projecting the features extracted from the samples of both domains into the linear subspace, we estimate their uncertainty based on the neighbors searching and find the known/unknown samples. We refine the label of known samples with the δ -filter and send all target samples into the classifiers with pseudo labels. Based on the prediction of unknown samples, we can compute the uncertainty-guided margin which balances the intra-class variances of both domains and leads to a reliable classification.

With the denoting that B_i is the smallest sphere containing $Z_i^s = \{\mathbf{z}'_1 \dots \mathbf{z}'_l\}$, where Z_i^s is the set of all source sample belong to class i , we assume that:

$$\forall i, j \in \{0, \dots, C\}; B_i \cap B_j = \emptyset \quad (8)$$

Then, we have:

$$\hat{p}(\mathbf{z}' \in U_{r_k}(\mathbf{z}) | \mathbf{z}' \in Z_i^s) = \frac{|U_{r_k}(\mathbf{z}) \cap B_i|}{|U_{r_k}(\mathbf{z})|} \quad (9)$$

We assume the number of neighbors is big enough. Then we have the estimation $|U_{r_k}(\mathbf{z}) \cap B_i| = c_0 \frac{k_i}{k}$ where c_0 is a constant. Then the approximation of $\hat{p}_i(\mathbf{z}; k)$ can be attained by:

$$\hat{p}_i(\mathbf{z}; k, k_i) = c_0 \frac{k_i}{k(r_k)^{m-1}} \quad (10)$$

where k_i is the number of samples belonging to U_{r_k} and B_i .

Then, another challenge of estimating $p(y \in Y^s | \mathbf{z})$ is computing p_{C+1} since we do not have a litter prior knowledge about unknown samples. The only knowledge we have is that samples not belonging to all the source classes belong to unknown class. Thus, we can attain:

$$\hat{p}_{C+1}(\mathbf{z}; k) = c_1 \mathbb{1}\left\{ \max_{i=0, \dots, C} \hat{p}_i(\mathbf{z}; k, k_i) \leq \beta \right\} \quad (11)$$

where β is a constant chosen to satisfy the equation.

Lemma 3 With assuming that $\hat{p}_{C+1}(\mathbf{z}; k)$ satisfies Eq. (11), we can infer Eq. (2) with the restriction Eq. (1)

Proof According to Eqs. (3), (4) and (5), with denoting $\sum_{i=0}^C p(y = j) = \epsilon$ and $k_{max} = \max_{i=0, \dots, C} (k_i)$, for a real number $\gamma \in [0, 1]$ we have:

If

$$c_0 \frac{k_{max}}{k(r_k)^{m-1}} \leq \beta \quad (12)$$

Then,

$$\begin{aligned} & \mathbb{1}\{p(y = C+1 | \mathbf{z}) < \gamma\} \\ &= \mathbb{1}\{1 - p(y \in Y^s | \mathbf{z}) > \gamma\} \\ &= \mathbb{1}\left\{ \frac{(1 - \epsilon) \hat{p}_{C+1}(\mathbf{z}; \mathbf{k})}{\epsilon \sum_{i=0}^C \hat{p}_i(\mathbf{z}; \mathbf{k}) + (1 - \epsilon) \hat{p}_{C+1}(\mathbf{z}; \mathbf{k})} > \gamma \right\} \\ &= \mathbb{1}\left\{ \frac{(1 - \epsilon)}{\frac{\epsilon c_0}{(r_k)^{m-1}} + (1 - \epsilon)} > \gamma \right\} \\ &= \mathbb{1}\left\{ (r_k)^{m-1} < \frac{\epsilon c_0 \gamma}{(1 - \gamma)(1 - \epsilon)} \right\} \end{aligned} \quad (13)$$

Plus, when $c_0 \frac{k_{max}}{k(r_k)^{m-1}} > \beta$, we have:

$$p(y = C+1 | \mathbf{z}) = 0 \quad (14)$$

Notably, in ODA problem [2], [11] where the source label set is contained in the target label set, we can get the equation:

$$p(y \in Y^s | \mathbf{z}) = p(y \in Y^{com} | \mathbf{z}) \quad (15)$$

We can estimate the probability of a target sample belonging to one of the common classes reliably based on Eqs. (4) and (5). However, in OPDA problem [16], [17], Eq. (15) would not work any more because of the private source classes existing.

Then, from the Proposition 1, when k_{max} satisfies Eq. (1), upper boundary of the probability $p(y = C+1 | \mathbf{z})$ is positive correlation with the k -nearest neighbor distance r_k , i.e., when k_{max} and r_k are big enough, the bigger r_k means the bigger probability of a target sample being unknown.

Corollary 4 In UniDA problem, a known target sample \mathbf{z} should satisfy the following conditions:

- The neighbors of \mathbf{z} should mostly belong to one of common classes.

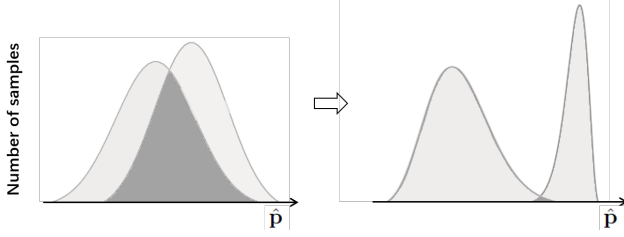


Fig. 3. Illustration for the effect of NSLS. Extracting the principal linear subspace can reduce the overlap of \hat{p} of known target samples and unknown target samples.

- \mathbf{z} should be close enough to its neighbors.

Base on the conditions mentioned in the Corollary 4, the reliable neighbors searching scheme is necessary because the domain misalignment can cause the mismatch between the target samples and the source samples.

3.3 Discovering Unknown Samples Based on the Uncertainty Estimation

To improve the neighbors searching scheme based on k -NN algorithm and discover unknown samples reliably, we propose an uncertainty estimation method to discover unknown samples, which is based on the neighbor searching in the linear subspace and a δ -filter to justify if a target sample can satisfy those two conditions respectively.

3.3.1 Neighbors searching in linear subspace (NSLS)

Since some unknown samples can distribute in the edges of clusters of source classes and the domain discrepancy may lead to some known samples far away from the centers of source classes, clustering target samples with their nearest neighbors or nearest prototypes is dangerous in the original feature space. Therefore, we propose to find a reliable linear subspace to deal with the above problems and improve the accuracy of the unknown samples discovering based on the neighborhood information searched from source domain. In specific, given $Z^s = [\mathbf{z}_0^s, \mathbf{z}_1^s, \dots, \mathbf{z}_{N_s}^s]^\top \in \mathbb{R}^{N_s \times m}$ and $\mathcal{B} = [\mathbf{z}_0^t, \mathbf{z}_1^t, \dots, \mathbf{z}_b^t]^\top \in \mathbb{R}^{b \times m}$, where m means the dimension of \mathbf{z}_i , Z^s and \mathcal{B} are sets of all source samples and target samples in a mini-batch respectively. We denote the original feature set $Z = [\mathbf{z}_0^s, \mathbf{z}_1^s, \dots, \mathbf{z}_n^s, \mathbf{z}_0^t, \mathbf{z}_1^t, \dots, \mathbf{z}_b^t] \in \mathbb{R}^{n \times m}$ where $n = N_s + b$.

Then, we have

$$Z_{sub} = ZP, P \in \mathbb{R}^{m \times p}, Z_{sub} \in \mathbb{R}^{n \times p} \quad (16)$$

where P is a transformation matrix mapping the features with m dimensions to reduced features with p dimensions.

To get the Z_{sub} , we propose to analyze the covariance matrix of Z . After centralize Z , the covariance matrix A can be defined as:

$$A = \frac{1}{n} Z Z^\top = [cov(\mathbf{z}_i, \mathbf{z}_j)]_{i,j=0,\dots,n}^{n \times n} \quad (17)$$

Inspired by Wang *et al.* [39], the covariance matrix captures the feature distribution of the training data, and contains rich information of potential semantic difference. We propose to decompose the covariance matrix A to find the dimensions which can mostly represent the difference on semantic information of each source class and cut off

the other dimensions. After the reduction of dimensions, since the unknown target samples do not share the common features with known source classes, the distances from an unknown sample to each source classes can be averaged which can lower k_{max} in Eq. (1). Specifically, we leverage the singular value decomposition (SVD) method to decompose the covariance matrix A :

$$A = U_{m \times m} \Sigma_{m \times m} V_{m \times m}, \quad (18)$$

Then, we can get the transformation matrix P from V :

$$P = V_{m \times p}^\top \quad (19)$$

By projecting the original features to the linear subspace, we propose to search neighbors of each target sample in the subspace. Particularly, we firstly employ a memory bank M to store all features of source samples:

$$M = [\mathbf{m}_0, \dots, \mathbf{m}_n] \quad (20)$$

with a momentum scheme to update the memory bank:

$$\mathbf{m}_i = \alpha \mathbf{m}_i + (1 - \alpha) \mathbf{z}_i \quad (21)$$

Then, we project the set $Z = [\mathbf{m}_0, \dots, \mathbf{m}_{N_s}, \mathbf{z}_0^t, \mathbf{z}_1^t, \dots, \mathbf{z}_b^t]$ to Z_{sub} . We search the neighbors \mathcal{N} for each target sample \mathbf{z}_i in Z_{sub} . We propose an uncertainty score of \mathbf{z}_i according to Eq.(10):

$$u(\mathbf{z}_i) = \max_{[i=0,\dots,Y]} (|\{\mathbf{z}' \in \mathcal{N}^k | y' = i\}|) \quad (22)$$

where k is the number of searched neighbors. Then, the discovered unknown samples are denoted as:

$$\hat{Z}^{unk} = \{\mathbf{z}_i | u(\mathbf{z}_i) \leq \tau\} \quad (23)$$

where τ is set manually. Similarly, the known samples are denoted as:

$$\hat{Z}^k = \{\mathbf{z}_i | u(\mathbf{z}_i) > \tau\} \quad (24)$$

and $\mathbf{z}_i \in \hat{Z}^k$ has pseudo label \hat{y}_i .

3.3.2 δ -filter for unknown samples discovering

As mentioned in the second condition in Corollary 4, the target sample should be close enough to its neighbors. However, the 'nearest' neighbors is not equivalent to 'most compact' neighbors. For instance, for an unknown sample, which is far away from from all source classes, its 'nearest' neighbors can also mostly belong to the same class. It means that there are some noisy data in \hat{Z}^k . Moreover, since known ones might also distribute on the edge of clusters of source classes, the distance from a centroid of a source class to a known sample might not be significantly different from the distance between the centroid and an unknown sample. Thus, it is hard to filter noisy known samples from \hat{Z}^k through the k -nearest neighbor distance. Therefore we introduce a dynamical δ -filter scheme to remove the noisy data.

To be specific, as shown in Fig. 4, compared to the compactness of the class \hat{y}_i , a credible known sample $\mathbf{z}_i \in \hat{Z}^k$ should be compact enough with its neighbors belonging to class \hat{y}_i . To estimate the compactness of \mathbf{z}_i and its neighbors, we apply the spectral decomposition on the covariance matrices of these vectors (i.e., \mathbf{z}_i and its neighbors belonging to class \hat{y}_i) to get the maximum eigenvalues of the covariance

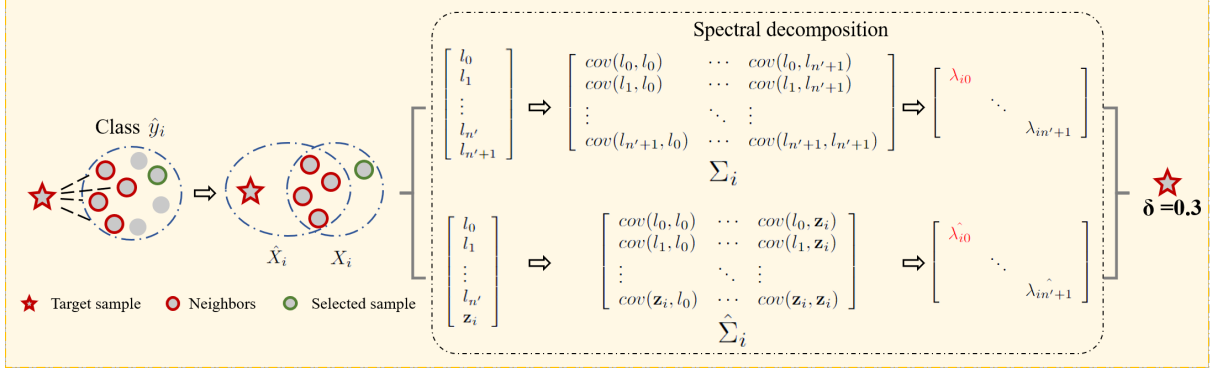


Fig. 4. Computation of δ : the target sample should be compact enough with its neighbors compared to the compactness of the source class.

matrices which can represent the dispersion of the vectors. Moreover, to get a comparable estimation of the dispersion of vectors in the class \hat{y}_i , we random select a sample from the source class \hat{y}_i which is not the neighbor of \mathbf{z}_i and compute the maximum eigenvalue of their covariance matrix (i.e., the selected vector and the neighbors belonging to class \hat{y}_i). We leverage the difference of the two eigenvalues to determine whether \mathbf{z}_i is noisy.

In detail, for $\mathbf{z}_i \in \hat{Z}^k$, we denote $\mathcal{N}'_i = \{l_0, l_1, \dots, l_{n'}\}$ as the neighbors of \mathbf{z}_i where samples in \mathcal{N}'_i belong to class \hat{y}_i and $n' = |\mathcal{N}'_i| > \tau$. Next, we can denote two zero-mean matrices defined as:

$$\begin{aligned} X_i &= \text{centralize}([l_0, l_1, \dots, l_{n'}, l_{n'+1}]), \\ \hat{X}_i &= \text{centralize}([l_0, l_1, \dots, l_{n'}, \mathbf{z}_i]) \end{aligned} \quad (25)$$

where $l_{n'+1}$ means the selected source sample. Then, we can get the covariance matrices of both sets:

$$\Sigma_i = \frac{1}{n'+1} X_i X_i^T, \quad \hat{\Sigma}_i = \frac{1}{n'+1} \hat{X}_i \hat{X}_i^T \quad (26)$$

We leverage spectral decomposition on both covariance matrices to get maximum eigenvalues λ_i and $\hat{\lambda}_i$ of Σ_i and $\hat{\Sigma}_i$ respectively. Finally, we define the difference value δ_i as:

$$\delta_i = |\lambda_i - \hat{\lambda}_i| \quad (27)$$

When δ_i is bigger, it means that connecting \mathbf{z}_i has significantly bad influence on the description of the vector set and \mathbf{z}_i should be filtered out from \hat{Z}^k . Based on the above analysis, we assume that a clean known target sample should satisfy $\delta_i \leq 0.2\lambda_i$.

3.4 Learning

With discovered unknown samples, we aim to train the classifier to categorize a target sample into one of the source classes with highly confidence and distinguish target samples belonging to the unknown class via the entropy of the output. Thus, the training of classifier D involves a trade-off: maximizing classification performance on Z^{com} and preventing overconfident predictions on Z^{unk} . With denoting $W = [W_0^T, W_1^T, \dots, W_{Y^s}^T]$ as the weights of linear classifier, a traditional method [7], [13], [14] is to improve the classification performance by training the classifier in the source domain with a cross-entropy loss:

$$\mathcal{L}_s = \frac{1}{n} \sum_{\mathbf{z}_i^s \in Z^s} -\log \frac{e^{W_{y_i}^T \mathbf{z}_i}}{e^{W_{y_i}^T \mathbf{z}_i} + \sum_{j \neq i} e^{W_j^T \mathbf{z}_i}} \quad (28)$$

Algorithm 1 Full algorithm of our method

Requirement:

Source dataset (Z^s, Y^s) , target dataset Z^t ,
The number of neighbors k and the threshold τ

Training:

while step < max step **do**

if step = 0 **do**

 Extract all features from Z^s and initial M

 Sample batch \mathcal{B}^s from (Z^s, Y^s) and batch \mathcal{B}^t from Z^t

 Extract features from each of \mathcal{B}^s and \mathcal{B}^t

for $\mathbf{z}_i^s \in \mathcal{B}^s$ **do**

 Update M by Eq.(21)

for $\mathbf{z}_i^t \in \mathcal{B}^t$ **do**

 Retrieve the nearest neighbors \mathcal{N}_i for \mathbf{z}_i^t from M

 Compute the uncertainty score $u(\mathbf{z}_i)$ as Eq. (22)

 Compute \sum_i and $\hat{\sum}_i$ by Eq. (26)

 Decompose \sum_i and $\hat{\sum}_i$ get λ_i and $\hat{\lambda}_i$

 Compute δ_i by Eq. (27)

if $u(\mathbf{z}_i^t) < \tau$ and $\delta \leq 0.2\lambda_i$ **do**

 Append \mathbf{z}_i^t into \hat{Z}^{unk}

else do

 Append \mathbf{z}_i^t into \hat{Z}^k

 Compute \mathcal{L}_{sup} based on Eq.(32)

 Compute the margin μ based on Eq.(30)

 Compute \mathcal{L}_{ugm} based on Eq.(29)

 Compute \mathcal{L}_{unk} based on Eq.(31)

 Compute the overall loss \mathcal{L}_{all}

 Update the model

where $W_{y_i}^T$ is the weight of class y_i which is the ground truth of \mathbf{z}_i^s .

However, this method can usually lead to the overconfident predictions on unknown samples [9]. To deal with the problem, Cao *et al.* [7] aggregated multiple complementary uncertainty measures, OVANet [13] employed an one-vs-all classifier for unknown samples classifying and GATE [9] proposed an energy-based classifier which extended the traditional softmax-based classifier to improve the classification performance on unknown samples. In this work, without applying extra parameters, we propose a more efficient method to train only one classifier via three losses.

3.4.1 Uncertainty-guided margin loss (UGM)

Since using the traditional CE loss training on source domain creates an imbalance problem between the known and unknown classes for target samples. Learning on source

classes Y^s is much faster than that on the unknown class Y^{unk} due to the supervised objective which lead the whole model to be biased towards the common classes Y^s in target domain. In result, the intra-class variance of source domain can be much smaller than that of target domain, including known target classes and the unknown class. The bias can cause the overconfident predictions for many unknown samples. Therefore, it is important to balance the intra-class variances of both domains. We propose a new uncertainty-guided margin loss (UGM) to achieve that. At the beginning of the training, we enforce a larger margin to encourage a larger intra-class variance which is similar to the intra-class variance of discovered unknown samples while the margin goes down to zero close to the end of the training,

$$\mathcal{L}_{ugm} = \frac{1}{n} \sum_{\mathbf{z}_i \in \mathcal{Z}_i} -\log \frac{e^{s(W_{y_i}^T \mathbf{z}_i + \alpha\mu)}}{e^{s(W_{y_i}^T \mathbf{z}_i + \alpha\mu)} + \sum_{j \neq y_i} e^{sW_j^T \mathbf{z}_i}} \quad (29)$$

where μ is the intra-class variance of \hat{Z}^{unk} which is defined as:

$$\mu = \frac{1}{|\hat{Z}^{unk}|} \sum_{\mathbf{z}_j \in \hat{Z}^{unk}} \max(0, \max_{k=0, \dots, C} p(y=k|\mathbf{z}_j) - \frac{1}{2}) \quad (30)$$

where $|\cdot|$ means the number of elements in a set. Notably, we normalize the weights and inputs, i.e., $W_{y_i}^T = \frac{W_{y_i}^T}{|W_{y_i}^T|}$ and $\mathbf{z}_i = \frac{\mathbf{z}_i}{|\mathbf{z}_i|}$.

3.4.2 Uniforming loss for unknown samples

Since we use the entropy of the classifier output to distinguish the unknown samples, we need to lower the confidence of unknown samples belonging to \hat{Z}^{unk} . We employ the uniforming loss to smooth posterior distribution for unknown inputs to increase the entropy:

$$\mathcal{L}_{unk} = -\frac{1}{2|\hat{Z}^{unk}|} \sum_{\mathbf{z}_i \in \hat{Z}^{unk}} \sum_{i=0}^Y \log D(\mathbf{z}) - \log Y \quad (31)$$

where the inputs of Eq.(31) belong to the discovered unknown samples set \hat{Z}^{unk} .

3.4.3 Supervised contrastive loss on source domain

Moreover, to reduce the influence of the domain misalignment, it is necessary to make each source class more compact and discriminative to enlarge the gap between two source classes which can improve the consistency of neighbors' labels for a known target sample when it searches the nearest neighbors from source domain. Thus, we employ a supervised contrastive learning loss [28] \mathcal{L}_{sup} to make data points in source domain more compact by pushing the samples from different classes away while pulling the samples from the same class closer. \mathcal{L}_{sup} is given by:

$$\mathcal{L}_{sup} = \frac{1}{|B^s|} \sum_{i=0}^{|B^s|} \frac{\sum_{\mathbf{m}_j \in \mathcal{A}_i^+} \exp(\langle \mathbf{z}_i, \mathbf{m}_j \rangle / t)}{\sum_{\mathbf{m}_j \in \mathcal{A}_i^- \cup \mathcal{A}_i^+} \exp(\langle \mathbf{z}_i, \mathbf{m}_j \rangle / t)} \quad (32)$$

where \mathcal{A}_i^+ and \mathcal{A}_i^- represent the positive samples in M with the same label as \mathbf{z}_i and the negative samples searched from M , respectively. t is a temperature parameter.

3.4.4 Total loss and algorithm

The total training loss of our method can be computed as

$$\mathcal{L}_{all} = \mathcal{L}_{ugm} + \lambda \mathcal{L}_{unk} + \mathcal{L}_{sup} \quad (33)$$

where λ is a weighting parameter. Moreover, the full algorithm of our method is provided in **Algorithm 1**.

4 EXPERIMENTAL RESULTS

In this section, we first introduce our experimental setups which includes datasets, evaluation protocols and training details. Then, we introduce some SOTA methods in UniDA and compare results in main datasets with them. We also conduct extensive ablation studies to demonstrate the effectiveness of each component of the proposed method. All experiments were implemented on one RTX2080Ti 11GB GPU with PyTorch 1.7.1 [41].

4.1 Experimental Setups

4.1.1 Datasets and evaluation protocols

We conduct experiments on four datasets. **Office-31** [42] consists of 4,652 images from three domains: DSLR (D), Amazon (A), and Webcam (W). **OfficeHome** [43] is a more challenging dataset, which consists of 15,500 images from 65 categories. It is made up of 4 domains: Artistic images (A), Clip-Art images (C), Product images (P), and Real-World images (R). **VisDA** [44] is a large-scale dataset, where the source domain contains 15,000 synthetic images and the target domain consists of 5,000 images from the real world.

In this paper, we use the **H-score** in line with recent UniDA methods [13], [14], [15]. H-score, proposed by Fu *et al.* [15], is the harmonic mean of the accuracy on the common classes a_{com} and the accuracy on the unknown class a_{unk} :

$$h = \frac{2a_{com}a_{unk}}{a_{com} + a_{unk}}. \quad (34)$$

4.1.2 Training details

We employ the ResNet-50 [45] backbone which is pre-trained on ImageNet [46] and optimize the model using Nesterov momentum SGD with momentum of 0.9 and weight decay of 5×10^{-4} . The batch size is set to 36 through all datasets for both domains. The initial learning rate is set as 0.01 for the classifier layers and 0.001 for the backbone layers. The learning rate is decayed with the inverse learning rate decay scheduling. The number of neighbors retrieved is set to be dependent on the sizes of the datasets. For Office-31 (4,652 images in 31 categories) and OfficeHome (15,500 images in 65 categories), the number of retrieved neighbors $|\mathcal{N}_i|$ is set to 10. For VisDA (20,000 images in total), we set $|\mathcal{N}_i|$ to 100, respectively. We set λ to 0.1 and t to 0.05 which are constant through all the datasets. In the test phase, the threshold of distinguishing the unknown samples is set to $\frac{\log C}{2}$ following DANCE [17] which used the entropy of the classifier's output to determine the unknown samples.

TABLE 1
Comparison of main results on Office31. Some results for previous methods are cited from OVANet [13] and GATE [18].

Method	OPDA (H-score)							ODA (H-score)						
	Office31 (10/10/11)							Office31 (10/5/50)						
	A2D	A2W	D2A	D2W	W2D	W2A	Avg	A2D	A2W	D2A	D2W	W2D	W2A	Avg
UAN [21]	59.7	58.6	60.1	70.6	71.4	60.3	63.5	38.9	46.8	68.0	68.8	53.0	54.9	55.1
CMU [15]	68.1	67.3	71.4	79.3	80.4	72.2	73.1	52.6	55.7	76.5	75.9	64.7	65.8	65.2
DANCE [17]	78.6	71.5	79.9	91.4	87.9	72.2	80.3	84.9	78.8	79.1	78.8	88.9	68.3	79.8
DCC [14]	88.5	78.5	70.2	79.3	88.6	75.9	80.2	58.3	54.8	67.2	89.4	80.9	85.3	72.6
ROS [16]	71.4	71.3	81.0	94.6	95.3	79.2	82.1	82.4	82.1	77.9	96.0	99.7	77.2	85.9
USFDA [40]	85.5	79.8	83.2	90.6	88.7	81.2	84.8	85.5	79.8	83.2	90.6	88.7	81.2	84.8
OVANet [13]	85.8	79.4	80.1	95.4	94.3	84.0	86.5	89.2	89.0	86.4	97.1	98.2	88.1	91.3
GATE [18]	87.7	81.6	84.1	94.8	94.1	83.4	87.6	88.4	86.5	84.2	95.0	96.7	86.1	89.5
Ours	87.3	83.5	82.2	96.1	99.2	84.7	88.8	91.9	88.8	86.9	94.8	99.7	86.7	91.5

TABLE 2
Comparison of main results on OfficeHome. Some results for previous methods are cited from OVANet [13] and GATE [18].

Open-partial Domain Adaptation Setting (H-score)															
Method	OfficeHome (10/5/50)													Visda(6/3/3)	
	A2C	A2P	A2R	C2A	C2P	C2R	P2A	P2C	P2R	R2A	R2C	R2P	Avg	S2R	
OSBP [11]	39.6	45.1	46.2	45.7	45.2	46.8	45.3	40.5	45.8	45.1	41.6	46.9	44.5	27.3	
UAN [21]	51.6	51.7	54.3	61.7	57.6	61.9	50.4	47.6	61.5	62.9	52.6	65.2	56.6	30.5	
CMU [15]	56.0	56.9	59.1	66.9	64.2	67.8	54.7	51.0	66.3	68.2	57.8	69.7	61.6	34.6	
DCC [14]	57.9	54.1	58.0	74.6	70.6	77.5	64.3	73.6	74.9	80.9	75.1	80.4	70.1	43.0	
OVANet [13]	62.8	75.6	78.6	70.7	68.8	75.0	71.3	58.6	80.5	76.1	64.1	78.9	71.8	53.1	
GATE [18]	63.8	75.9	81.4	74.0	72.1	79.8	74.7	70.3	82.7	79.1	71.5	81.7	75.6	56.4	
Ours	64.5	77.9	87.1	74.1	71.0	78.1	74.2	70.0	84.1	80.2	71.5	86.2	76.6	55.3	

Open-set Domain Adaptation Setting (H-score)															
Method	OfficeHome (25/0/40)													Visda(6/0/6)	
	A2C	A2P	A2R	C2A	C2P	C2R	P2A	P2C	P2R	R2A	R2C	R2P	Avg	S2R	
OSBP [2]	55.1	65.2	72.9	64.3	64.7	70.6	63.2	53.2	73.9	66.7	54.5	72.3	64.7	52.3	
ROS [16]	60.1	69.3	76.5	58.9	65.2	68.6	60.6	56.3	74.4	68.8	60.4	75.7	66.2	66.5	
UAN [21]	40.3	41.5	46.1	53.2	48.0	53.7	40.6	39.8	52.5	53.6	43.7	56.9	47.5	51.9	
CMU [15]	61.9	61.3	63.7	64.2	58.6	62.6	67.4	61.0	65.5	65.9	61.3	64.2	63.0	67.5	
DCC [14]	56.1	67.5	66.7	49.6	66.5	64.0	55.8	53.0	70.5	61.6	57.2	71.9	61.7	59.6	
OVANet [13]	58.9	66.0	70.4	62.2	65.7	67.8	60.0	52.6	69.7	68.2	59.1	67.6	64.0	66.1	
GATE [18]	63.8	70.5	75.8	66.4	67.9	71.7	67.3	61.5	76.0	70.4	61.8	75.1	69.1	70.8	
Ours	62.5	79.1	80.9	72.2	71.7	78.5	73.6	61.8	84.5	79.1	65.7	82.8	74.4	74.5	

4.2 Comparison With the SOTA Methods

4.2.2 Results in main datasets

4.2.1 Baselines

We aim to show that our method can better balance the confidences of known and unknown samples for UniDA by comparing our method with the current SOTA methods, such as UAN [21] and DANCE [17], which employed a softmax-based classifier to produce the confidence of each sample to determine whether it belongs to the unknown class or not. Also, we compare our method with DANCE [17], DCC [13] and GATE [18] to show that it is more effect to adapt the domain misalignment through the dimensional reduction rather than completing it in the original feature space.

TABLE 1 lists the results on Office-31 with OPDA setting and ODA setting respectively. TABLE 2 lists the results on OfficeHome and Visda both with OPDA setting and ODA setting, respectively. On Office-31, our method outperforms the SOTA methods by 1.2% in terms of the H-score on average with OPDA setting and made a significant improvement of 2.0% in terms of the H-score on average with ODA setting. For the more challenging dataset OfficeHome which contains much more private classes than common classes, our method also made a significant improvement of 1.0% in terms of the H-score. Our method consistently performs better than other methods. VisDA is a much larger dataset than Office-31 and OfficeHome which contains about 10000 images in each domain.

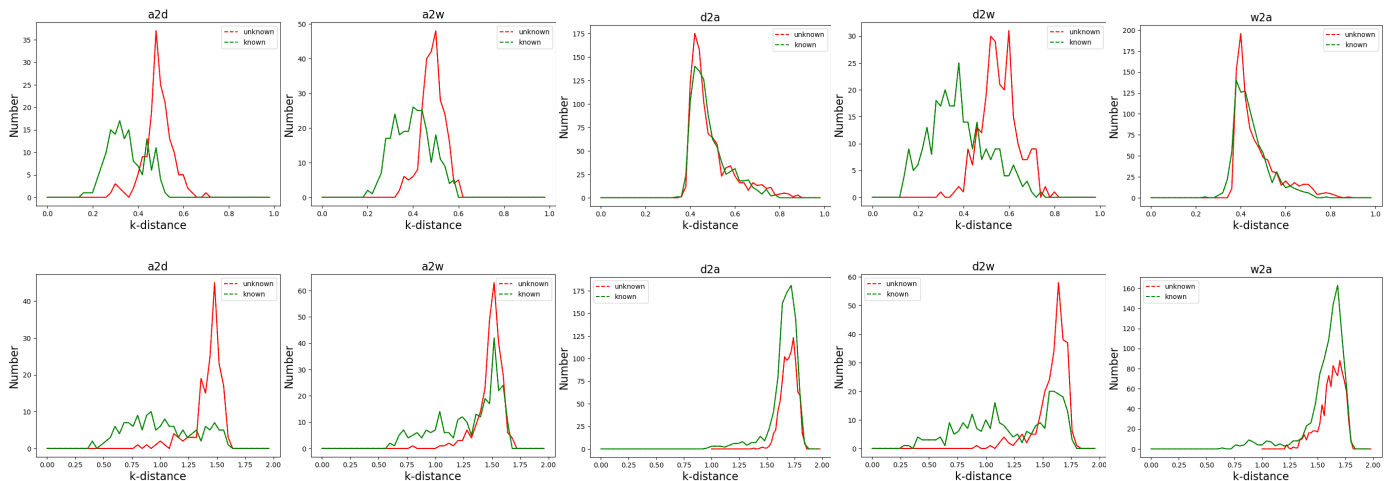


Fig. 5. Graphs of distributions of k -nearest neighbor distances of target samples in an early epoch on Office-31 with the OPDA setting. The red lines represent the distribution of unknown target samples while the green lines represent that of known target samples.

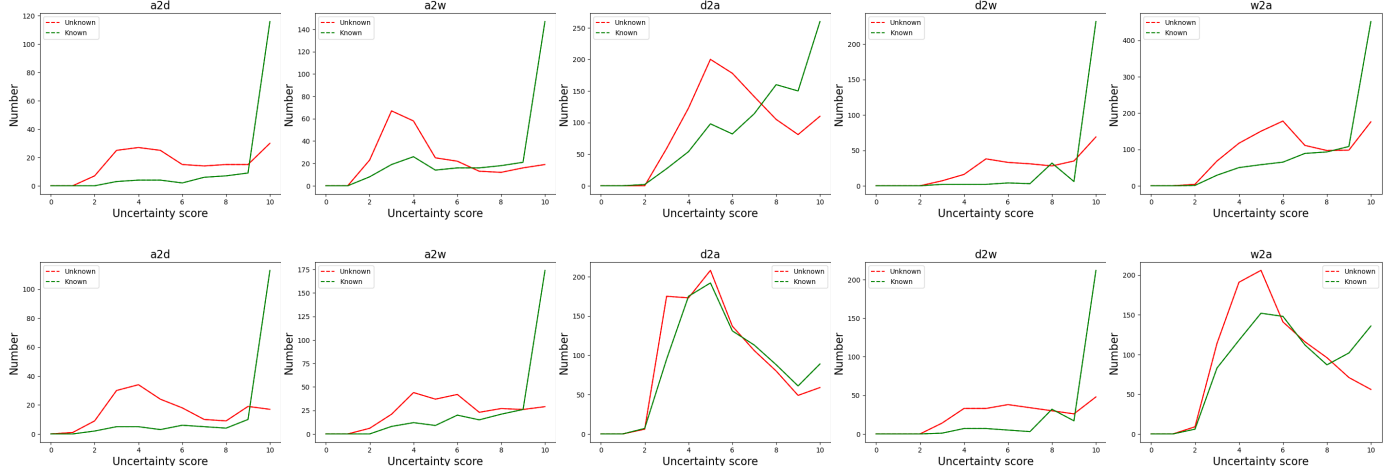


Fig. 6. Graphs of distributions of the maximum numbers of neighbors belonging to the same class of target samples in an early epoch on Office-31 with the OPDA setting. The red lines represent the distribution of unknown target samples while the green lines represent that of known target samples.

4.2.3 Summary

According to the results of quantitative comparisons, our method achieves the SOTA performance in every dataset and most subtasks, which demonstrates the main idea of our method that adapt the domain misalignment through dimensional reduction and balance the confidences of known and unknown samples by controlling the gradient updating of learning on the source domain.

4.3 Ablation Studies

4.3.1 A closer look at the unknown samples discovering

By Proposition 1, the posterior probability of a target sample belonging to the unknown class depends on the biggest number of neighbors belonging to the same class. Thus, we compare the proposed unknown samples discovering scheme with the discovering method based on the k -nearest neighbor distance in this part. First, we collect the k -nearest neighbor distances of all target samples in an early epoch in Office-31 which can be more influential for the whole training. As shown in the first row in Fig. 5, the distributions of known samples are not distinguishable enough especially in A2W, D2A and W2A. It is obvious that the k -nearest neighbor distance is not reliable enough

to discover the unknown samples. Moreover, the optimal thresholds for each subtasks are different and hard to choose. Notably, mapping samples into the linear subspace has the significant influence in uniforming the distribution of data points and make them more sparse as shown in the second row in Fig. 5. However, it is helpless to improve the discrimination of unknown samples based on the k -nearest neighbor distance. By contrast, the distributions of confidences defined by the biggest number of neighbors belonging to the same class illustrated in the first row of Fig. 6 are much more distinguishable.

4.3.2 Justification of unknown samples discovering based on the uncertainty estimation

Original feature space VS Linear subspace. The purpose of extracting a linear subspace is to make the distribution of data points more sparse and uniform to avoid the influence of the domain misalignment. Comparing the charts in the first row and the second row in Fig. 5, it is obviously that the data points in the subspace are similar in the distribution of the k -nearest neighbor distances. In Fig. 6, we conduct experiments on Office-31 to compare the distributions of the confidences produced by the proposed unknown samples discovering method in the original

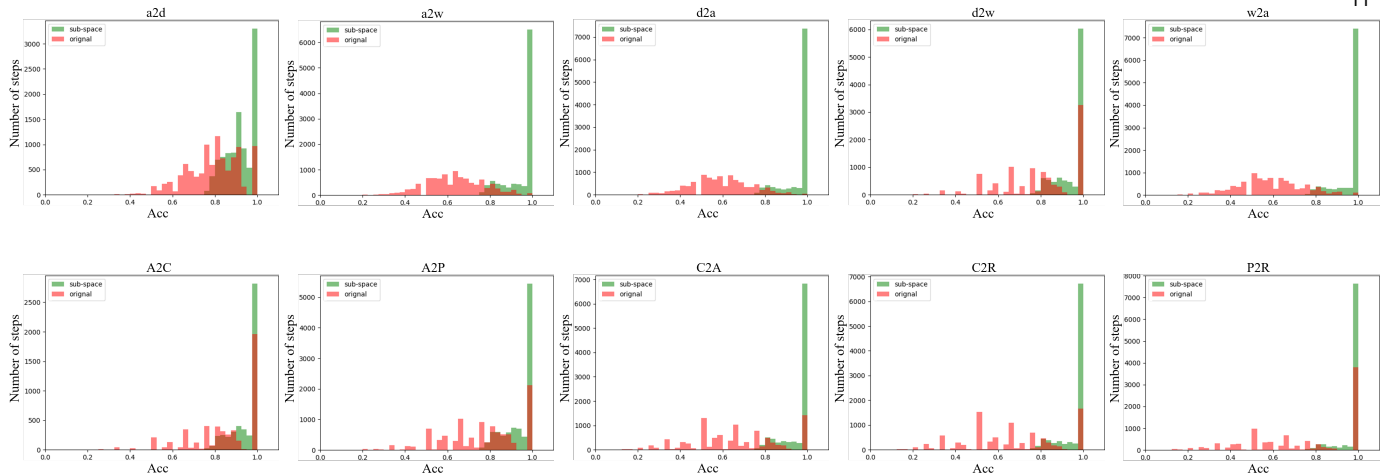


Fig. 7. Histograms of accuracy of unknown samples discovering in the original feature space (red columns) and in the subspace (green columns) on Office-31 (A2D, A2W, D2A, D2W and W2A) and OfficeHome (A2C, A2P, C2A, C2R and P2R) with the OPDA setting.

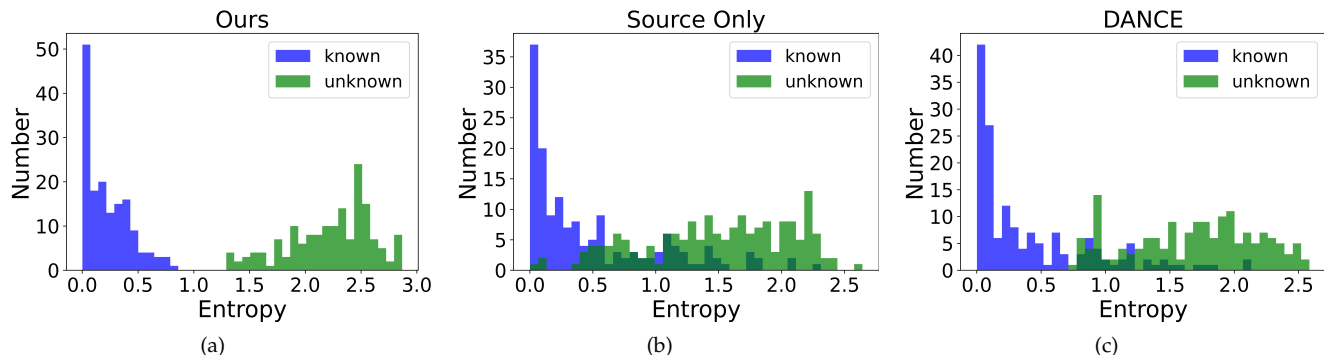


Fig. 8. Comparison on the distribution of the entropy. The three plots of histograms show the entropy at the last epoch produced by the full version of our method, the model trained only on source domain, and the model trained on DANCE [17] in Office-31(A2D) respectively. Each area in dark green indicates that there is an overlap between the green and the blue bars.

feature space (First row) and the linear subspace (Second row). Apparently, the distributions of confidences in the subspace are much more distinguishable than that in the original feature space where the overlaps between unknown and known samples are much fewer in the subspace which is benefited by reducing the misalignment between target samples and source samples.

Accuracy of the uncertainty estimation. We also conduct experiments on the accuracy of the uncertainty estimation on the original feature space and the subspaces with different dimensions on some subtasks of Office-31 and OfficeHome where we plot the histograms of the accuracy of the unknown samples discovering in Fig. 7. The accuracy unknown samples is consistently detected with high accuracy which far surpasses 80% on average and the performance of accuracy of unknown samples discovering method based on the uncertainty estimation in the subspace is much better than that in the original feature space. Thus, through the proposed unknown samples discovering scheme, our approach finds the unknown samples in the target domain reliably.

Quantitative comparison with different methods. To show the improvement on the distribution of the entropy which is used to classify the unknown samples in the test stage, we conducted experiments on Office-31(A2D). First, we plot the distributions of the entropies of all sample in the

target domain at the final epoch in Fig. 8(a). Then, we compare the plot to that trained on the source domain only in Fig. 8(b). We can observe that the full version of our method better distinguishes the known samples from the unknown ones. Furthermore, in Fig. 8(c), we show the corresponding plot produced by DANCE [17] for comparison. Noticeably, our method performs better than DANCE [17] in terms of distinguishing the known samples from the unknown ones.

4.3.3 Effect of losses

Uncertainty-guided margin loss VS CE-loss. To show the effect of the uncertainty-guided margin loss on balancing the predictions of known and unknown samples, we track the entropy level of unknown samples and the confidence level of known samples following the training process on Office-31. We recorded the mean value of entropies of predictions for unknown samples and the mean value of maximum prediction confidences output by the classifier of each known samples in every steps. For comparison, we first plot records where the classifier was only trained on source domain with a traditional CE-loss like Eq. 28 in the first row of Fig. 9. We can observe that although the known samples have high confidence consistently, most of unknown samples are significantly overconfident during the training process. In the second row of Fig. 6, we plot the records using the CE-loss and proposed uniforming loss

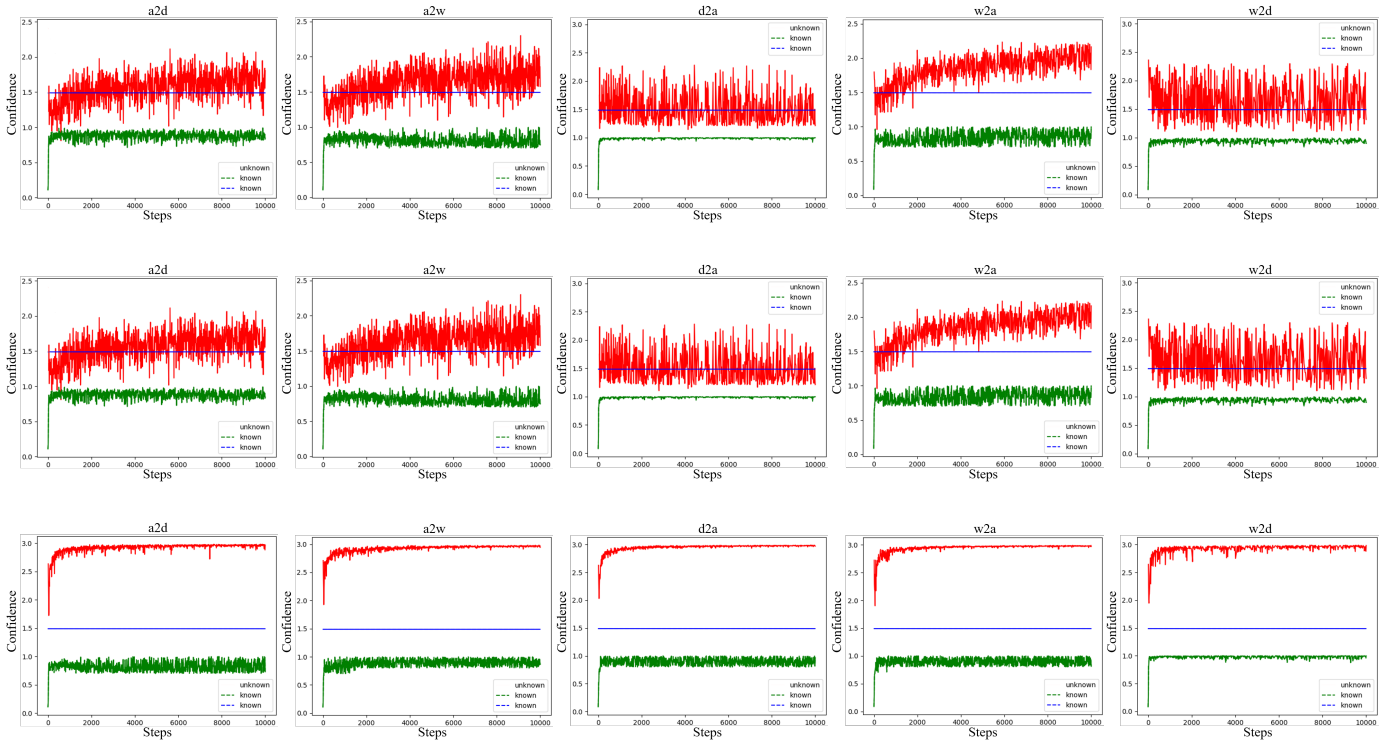


Fig. 9. Records of entropy of predictions of unknown samples and the maximum values of predictions of known samples following the training process on Office-31 with the OPDA setting. The red lines represent the record of unknown target samples while the green lines represent that of known target samples.

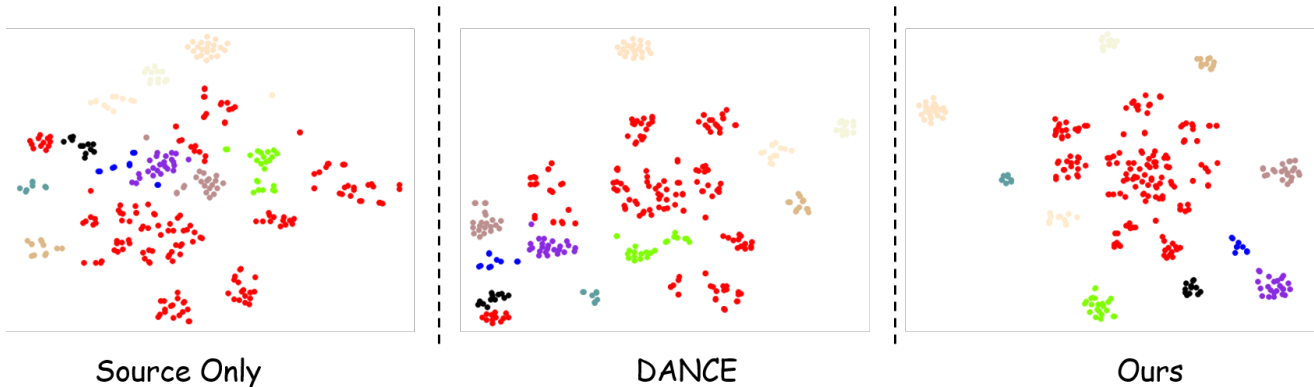


Fig. 10. The t-SNE visualizing cooperation. Different colors represent different classes. Red points represent the unknown samples while the points in other colors represent the known samples of different classes.

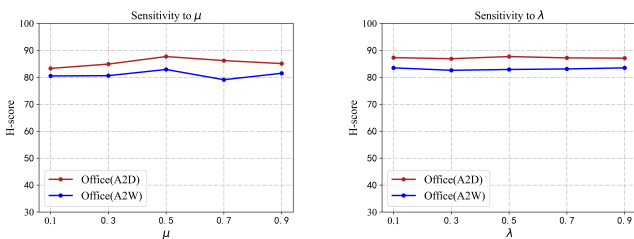


Fig. 11. (a) Results of different human-picked margins in terms of H-score. (b) Sensitivity to λ in terms of H-score.

as Eq. 31. The entropy level has been improved but the overconfidence of unknown samples is still obvious. In the third row of Fig. 9, we plot the records using the proposed uncertainty-guided loss which can perfectly distinguish the unknown samples with entropy while keeping the known samples with highly confident predictions. We also employ

t-SNE [47] pictures to visualize the distributions of target samples in Fig. 10. We can observe that the distribution of data points in ours (right) is much more discriminative than that of DANCE [17](mid) and the model training with the source dataset only (left).

Setting of uncertainty-guided margin. To show the effect of the uncertainty-guided margin selection scheme, we compare it with the human-picked thresholds on Office-31(A2D and D2A). From Fig. 11(a), we can observe that it is difficult to choose a consistently optimal threshold for all datasets and subtasks as the model is sensitive to the thresholds.

Different ablated versions of our method. Finally, we also provide an ablation study to investigate the effect of each loss in our UniDA framework and show the results in TABLE 3. We can see that all losses contribute to the

TABLE 3

Results of different ablated versions of our method on Office-31.

Method	Office-31 (10/10/11)						Avg
	A2D	A2W	D2A	D2W	W2D	W2A	
w/o \mathcal{L}_{ugm}	29.2	33.4	31.3	52.5	44.2	27.9	36.4
w/o \mathcal{L}_{unk}	81.0	77.5	78.2	95.0	91.0	72.9	82.6
w/o \mathcal{L}_{sup}	86.9	76.6	84.4	91.4	93.3	85.6	86.3
Ours	87.3	83.5	82.2	96.1	99.2	84.7	88.8

TABLE 4

Results on Office-31 using the VGGNet [48] backbone with the ODA setting.

Method	Office-31 (10/10/11)						Avg
	A2D	A2W	D2A	D2W	W2D	W2A	
OSBP [11]	81.0	77.5	78.2	95.0	91.0	72.9	82.6
ROS [16]	79.0	81.0	78.1	94.4	99.7	74.1	84.4
OVANet [13]	89.5	84.9	89.7	93.7	85.8	88.5	88.7
Ours	89.4	85.6	92.4	94.5	90.5	92.2	90.8

improvement of the results. In particular, among the three target-domain losses, both \mathcal{L}_{ugm} and \mathcal{L}_{unk} has the large impact on the final performance, which demonstrates that it is very important to balance the predictions of known/unknown samples.

4.3.4 Performance on VGGNet

TABLE 4 shows the quantitative comparison with the ODA setting on Office-31 using VGGNet [48] instead of ResNet-50 as the backbone for feature extraction. According to the results, we demonstrate that our method is also effective with another backbone without changing any hyper-parameters.

4.3.5 Sensitivity to λ

There is only one hyper-parameter λ in the loss items. To show the sensitivity of λ in the total loss, we conducted experiments on Office-31(A2D and D2A) with the UniDA setting. Fig. 11(b) shows that our method has a highly stable performance over different values of λ .

5 CONCLUSION

In this paper, we propose a new framework to reduce the influence of the domain misalignment and balance the predictions of known and unknown target samples. Its core idea is to estimate the probabilities of target samples belonging to the unknown class by the biggest number of neighbors with the same label searched from the source domain and detect the unknown samples via mapping the features in the original feature space into a linear subspace to make the data points more sparse and discriminative which can reduce the influence of domain misalignment. Also, our method well balance the confidences of known target samples and unknown target samples via an uncertainty-guided margin loss. As demonstrated by extensive experiments, our method sets the new SOTA performance in various subtasks on four public datasets.

REFERENCES

- [1] Y. Ganin and V. Lempitsky, "Unsupervised domain adaptation by backpropagation," in *International conference on machine learning*. PMLR, 2015, pp. 1180–1189.
- [2] K. Saito, K. Watanabe, Y. Ushiku, and T. Harada, "Maximum classifier discrepancy for unsupervised domain adaptation," in *Proceedings of the IEEE conference on computer vision and pattern recognition*, 2018, pp. 3723–3732.
- [3] M. Long, H. Zhu, J. Wang, and M. I. Jordan, "Unsupervised domain adaptation with residual transfer networks," *arXiv preprint arXiv:1602.04433*, 2016.
- [4] B. Gong, K. Grauman, and F. Sha, "Connecting the dots with landmarks: Discriminatively learning domain-invariant features for unsupervised domain adaptation," in *International Conference on Machine Learning*. PMLR, 2013, pp. 222–230.
- [5] Y. Zou, Z. Yu, B. Kumar, and J. Wang, "Unsupervised domain adaptation for semantic segmentation via class-balanced self-training," in *Proceedings of the European conference on computer vision (ECCV)*, 2018, pp. 289–305.
- [6] Z. Cao, L. Ma, M. Long, and J. Wang, "Partial adversarial domain adaptation," in *Proceedings of the European Conference on Computer Vision (ECCV)*, 2018, pp. 135–150.
- [7] Z. Cao, K. You, M. Long, J. Wang, and Q. Yang, "Learning to transfer examples for partial domain adaptation," in *Proceedings of the IEEE/CVF Conference on Computer Vision and Pattern Recognition*, 2019, pp. 2985–2994.
- [8] J. Zhang, Z. Ding, W. Li, and P. Ogunbona, "Importance weighted adversarial nets for partial domain adaptation," in *Proceedings of the IEEE conference on computer vision and pattern recognition*, 2018, pp. 8156–8164.
- [9] J. Liang, Y. Wang, D. Hu, R. He, and J. Feng, "A balanced and uncertainty-aware approach for partial domain adaptation," in *Computer Vision—ECCV 2020: 16th European Conference, Glasgow, UK, August 23–28, 2020, Proceedings, Part XI 16*. Springer, 2020, pp. 123–140.
- [10] P. Panareda Busto and J. Gall, "Open set domain adaptation," in *Proceedings of the IEEE International Conference on Computer Vision*, 2017, pp. 754–763.
- [11] K. Saito, S. Yamamoto, Y. Ushiku, and T. Harada, "Open set domain adaptation by backpropagation," in *Proceedings of the European Conference on Computer Vision (ECCV)*, 2018, pp. 153–168.
- [12] H. Liu, Z. Cao, M. Long, J. Wang, and Q. Yang, "Separate to adapt: Open set domain adaptation via progressive separation," in *Proceedings of the IEEE/CVF Conference on Computer Vision and Pattern Recognition*, 2019, pp. 2927–2936.
- [13] K. Saito and K. Saenko, "Ovanet: One-vs-all network for universal domain adaptation," *arXiv preprint arXiv:2104.03344*, 2021.
- [14] G. Li, G. Kang, Y. Zhu, Y. Wei, and Y. Yang, "Domain consensus clustering for universal domain adaptation," in *IEEE/CVF Conference on Computer Vision and Pattern Recognition (CVPR)*, 2021.
- [15] B. Fu, Z. Cao, M. Long, and J. Wang, "Learning to detect open classes for universal domain adaptation," in *European Conference on Computer Vision*. Springer, 2020, pp. 567–583.
- [16] S. Bucci, M. R. Loghmani, and T. Tommasi, "On the effectiveness of image rotation for open set domain adaptation," in *European Conference on Computer Vision*. Springer, 2020, pp. 422–438.
- [17] K. Saito, D. Kim, S. Sclaroff, and K. Saenko, "Universal domain adaptation through self supervision," *arXiv preprint arXiv:2002.07953*, 2020.
- [18] L. Chen, Y. Lou, J. He, T. Bai, and M. Deng, "Geometric anchor correspondence mining with uncertainty modeling for universal domain adaptation," in *Proceedings of the IEEE/CVF Conference on Computer Vision and Pattern Recognition*, 2022, pp. 16 134–16 143.
- [19] Z. Cao, M. Long, J. Wang, and M. I. Jordan, "Partial transfer learning with selective adversarial networks," in *Proceedings of the IEEE conference on computer vision and pattern recognition*, 2018, pp. 2724–2732.
- [20] Q. Feng, G. Kang, H. Fan, and Y. Yang, "Attract or distract: Exploit the margin of open set," in *Proceedings of the IEEE/CVF International Conference on Computer Vision*, 2019, pp. 7990–7999.
- [21] K. You, M. Long, Z. Cao, J. Wang, and M. I. Jordan, "Universal domain adaptation," in *Proceedings of the IEEE/CVF conference on computer vision and pattern recognition*, 2019, pp. 2720–2729.
- [22] I. Golan and R. El-Yaniv, "Deep anomaly detection using geometric transformations," *Advances in neural information processing systems*, vol. 31, 2018.

- [23] S. Wang, Y. Zeng, X. Liu, E. Zhu, J. Yin, C. Xu, and M. Kloft, "Effective end-to-end unsupervised outlier detection via inlier priority of discriminative network," *Advances in neural information processing systems*, vol. 32, 2019.
- [24] K. Lee, K. Lee, H. Lee, and J. Shin, "A simple unified framework for detecting out-of-distribution samples and adversarial attacks," *Advances in neural information processing systems*, vol. 31, 2018.
- [25] S. Pidhorskyi, R. Almohsen, and G. Doretto, "Generative probabilistic novelty detection with adversarial autoencoders," *Advances in neural information processing systems*, vol. 31, 2018.
- [26] S. Liang, Y. Li, and R. Srikant, "Enhancing the reliability of out-of-distribution image detection in neural networks," *arXiv preprint arXiv:1706.02690*, 2017.
- [27] D. Hendrycks and K. Gimpel, "A baseline for detecting misclassified and out-of-distribution examples in neural networks," *arXiv preprint arXiv:1610.02136*, 2016.
- [28] Q. Yu and K. Aizawa, "Unsupervised out-of-distribution detection by maximum classifier discrepancy," in *Proceedings of the IEEE/CVF international conference on computer vision*, 2019, pp. 9518–9526.
- [29] D. Hendrycks, M. Mazeika, S. Kadavath, and D. Song, "Using self-supervised learning can improve model robustness and uncertainty," *Advances in neural information processing systems*, vol. 32, 2019.
- [30] A. Vyas, N. Jammalamadaka, X. Zhu, D. Das, B. Kaul, and T. L. Willke, "Out-of-distribution detection using an ensemble of self supervised leave-out classifiers," in *Proceedings of the European Conference on Computer Vision (ECCV)*, 2018, pp. 550–564.
- [31] K. Lee, H. Lee, K. Lee, and J. Shin, "Training confidence-calibrated classifiers for detecting out-of-distribution samples," *arXiv preprint arXiv:1711.09325*, 2017.
- [32] J. Ren, P. J. Liu, E. Fertig, J. Snoek, R. Poplin, M. Depristo, J. Dillon, and B. Lakshminarayanan, "Likelihood ratios for out-of-distribution detection," *Advances in neural information processing systems*, vol. 32, 2019.
- [33] G. Shalev, Y. Adi, and J. Keshet, "Out-of-distribution detection using multiple semantic label representations," *Advances in Neural Information Processing Systems*, vol. 31, 2018.
- [34] Y.-C. Hsu, Y. Shen, H. Jin, and Z. Kira, "Generalized odin: Detecting out-of-distribution image without learning from out-of-distribution data," in *Proceedings of the IEEE/CVF Conference on Computer Vision and Pattern Recognition*, 2020, pp. 10951–10960.
- [35] Z. Liu, Z. Miao, X. Zhan, J. Wang, B. Gong, and S. X. Yu, "Large-scale long-tailed recognition in an open world," in *Proceedings of the IEEE/CVF Conference on Computer Vision and Pattern Recognition*, 2019, pp. 2537–2546.
- [36] L. Neal, M. Olson, X. Fern, W.-K. Wong, and F. Li, "Open set learning with counterfactual images," in *Proceedings of the European Conference on Computer Vision (ECCV)*, 2018, pp. 613–628.
- [37] R. Yoshihashi, W. Shao, R. Kawakami, S. You, M. Iida, and T. Naemura, "Classification-reconstruction learning for open-set recognition," in *Proceedings of the IEEE/CVF Conference on Computer Vision and Pattern Recognition*, 2019, pp. 4016–4025.
- [38] D. Mandal, S. Narayan, S. K. Dwivedi, V. Gupta, S. Ahmed, F. S. Khan, and L. Shao, "Out-of-distribution detection for generalized zero-shot action recognition," in *Proceedings of the IEEE/CVF Conference on Computer Vision and Pattern Recognition*, 2019, pp. 9985–9993.
- [39] Y. Wang, G. Huang, S. Song, X. Pan, Y. Xia, and C. Wu, "Regularizing deep networks with semantic data augmentation," *IEEE Transactions on Pattern Analysis and Machine Intelligence*, 2021.
- [40] J. N. Kundu, N. Venkat, R. V. Babu *et al.*, "Universal source-free domain adaptation," in *Proceedings of the IEEE/CVF Conference on Computer Vision and Pattern Recognition*, 2020, pp. 4544–4553.
- [41] A. Paszke, S. Gross, F. Massa, A. Lerer, J. Bradbury, G. Chanan, T. Killeen, Z. Lin, N. Gimelshein, L. Antiga *et al.*, "Pytorch: An imperative style, high-performance deep learning library," *Advances in neural information processing systems*, vol. 32, pp. 8026–8037, 2019.
- [42] K. Saenko, B. Kulis, M. Fritz, and T. Darrell, "Adapting visual category models to new domains," in *European conference on computer vision*. Springer, 2010, pp. 213–226.
- [43] X. Peng, Q. Bai, X. Xia, Z. Huang, K. Saenko, and B. Wang, "Moment matching for multi-source domain adaptation," in *Proceedings of the IEEE/CVF International Conference on Computer Vision*, 2019, pp. 1406–1415.
- [44] X. Peng, B. Usman, N. Kaushik, J. Hoffman, D. Wang, and K. Saenko, "Visda: The visual domain adaptation challenge," *arXiv preprint arXiv:1710.06924*, 2017.
- [45] K. He, X. Zhang, S. Ren, and J. Sun, "Deep residual learning for image recognition," in *Proceedings of the IEEE conference on computer vision and pattern recognition*, 2016, pp. 770–778.
- [46] J. Deng, W. Dong, R. Socher, L.-J. Li, K. Li, and L. Fei-Fei, "Imagenet: A large-scale hierarchical image database," in *2009 IEEE conference on computer vision and pattern recognition*. Ieee, 2009, pp. 248–255.
- [47] L. Van der Maaten and G. Hinton, "Visualizing data using t-sne." *Journal of machine learning research*, vol. 9, no. 11, 2008.
- [48] K. Simonyan and A. Zisserman, "Very deep convolutional networks for large-scale image recognition," *arXiv preprint arXiv:1409.1556*, 2014.